1Pa1-1

Computing SAW velocities using the matrix method and the Sakurai-Sugiura method

マクトリクス法と Sakurai-Sugiura 法による SAW 速度の計算

Hibiki Yoshida† and Koji Hasegawa (Grad. School Eng., Muroran Institute of Technology)

吉田 響†，長谷川 弘治 (室工大院)

1. Introduction

For computing propagation constants of surface acoustic waves (SAWs) and Leaky SAWs in multilayered piezoelectric substrate, we can use the matrix method[1,2] and finite element analysis of admittance characteristics of infinite interdigital transducers on the substrate. However, these methods cannot compute the number of eigenmodes in the specified velocity interval.

In this paper, we demonstrated computing SAW velocities and the number of eigenmodes in the specified disk region on the complex inverse velocity plane using the matrix method with two contour integral methods[3,4] that compute eigenvalues and the number of eigenvalues for a nonlinear eigenvalue problem (NEP) derived from the matrix method. Because the matrix of the NEP in the contour integral methods must be analytic, we presented an algorithm of choosing proper partial waves. Computed results of θ°rot. *Y-X* $\mathrm{LiNbO_3}$ substrate show the validity of the algorithm.

2. Nonlinear eigenvalue problems in the matrix method for SAW substrate

We consider SAWs propagating along the x-axis with the propagation constant β in a half-infinite substrate $(y \leq 0)$ and vacuum $(0 \leq y)$ without variation in the field distributions along the z-axis:

$$\vec{u}(x,y,t) = \vec{V}(y)\vec{G}\exp j(\omega t - \beta x), \tag{1}$$

$$\vec{u} = \left[u_x\ u_y\ u_z\ \phi\right]^{\mathrm{t}}, \tag{2}$$

$$\vec{V}(y) = [V_1(y), V_2(y), V_3(y), V_4(y)]^{\mathrm{t}}, \tag{3}$$

$$V_n(y) = \vec{A}_n \exp\left(-jk_{yn}y\right), \tag{4}$$

$$\vec{G} = [G_1\ G_2\ G_3\ G_4]^{\mathrm{t}}. \tag{5}$$

Here, ω is the angular frequency, $u_l\ (l = x, y, z)$ is the l-component of the particle displacement, ϕ is the electric potential, the superscript t of a matrix denotes the transpose of the matrix, k_{yn} and $\vec{A}_n$ $(n = 1,2,3,4)$ are four proper eigenvalues and eigenvectors of the christoffel equation for satisfying the radiation condition in the -y-axis as follows:

$$\left\{B_2\left(\frac{k_y}{\omega}\right)^2 + B_1\left(\frac{k_y}{\omega}\right) + B_0\right\}\vec{A} = \vec{0}, \tag{6}$$

where the entries of $B_i \in \mathbb{C}^{4\times4}\ (i = 0, 1, 2)$ are composed of material constants of the substrate and β.

Choosing a point $(0, y_0)$ and solving (1) for $\vec{G}$, we have

$$\vec{u}(x,y,t) = \mathrm{V}(y)\left(\mathrm{V}(y_0)\right)^{-1}\vec{u}(x,y_0,t). \tag{7}$$

Here, $^\forall y_0 \leq 0$. We can choose $y_0 = 0$ for numerical simplicity.

Computing strain componets T_{ly} and an electric displacement component D_y with the piezoelectric stress equations and (7), and appling boundary conditions in the substrate surface to the fields, we have an NEP for eigenvalue β/ω and eigenvector $\vec{u}(0, y_{,0}, 0)$:

$$T(\beta/\omega)\vec{u}(0, y_0, 0) = \vec{0}, \tag{8}$$

where $T \in \mathbb{C}^{4\times4}$. We can solve the NEP (8) using Sakurai-Sugiura method (SSM).

3. Computing the number of eigenvalues

Applying the argument principle to the NEP and approximating integrals along a circle with the center o and the radius ρ as numerical integrals using trapezoidal rule, we can compute the number of eigenvalues $\widehat{M}_{\mathrm{eig}}$ in the circle:

$$\widehat{M}_{\mathrm{eig}} = \sum_{c=0}^{N_s} w_c \mathrm{tr}\left(\left[T\left(\frac{\beta}{\omega}\right)\right]^{-1} \left.\frac{d\left[T\left(\frac{\beta}{\omega}\right)\right]}{d\left(\frac{\beta}{\omega}\right)}\right|_{\left(\frac{\beta}{\omega}\right)=\left(\frac{\beta}{\omega}\right)_c}\right), \tag{9}$$

where N_{s} is the number of sampling points, the operator tr denotes the trace of the matrix, $(\beta/\omega)_c = o + \rho\exp(j2\pi(c + 1/2)/N_s)$ [s/m], and $w_c = \rho/N_s \exp(j2\pi(c + 1/2)/N_s)$.

4. Algorithm for choosing proper partial waves in the substrate

In the substrate, (6) gives eight eigenvalues and we have to choose proper partial waves for computing $T(\beta/\omega)$ of (8) along the integral path in the SSM and (9).

For Leaky SAWs propagating faster than the slow quasishear bulk wave, we choose one propagating wave and three attenuation waves in the -y-axis: first we choose the partial wave with the minimum value of the y-component of the real part of the complex Poynting's vector P_y for the radiating wave along the integral path. Next, we choose three attenuation waves with $\mathrm{Im}(k_{yn}/\omega) > 0$. For LSAWs propagating slower than the slow quasishear bulk wave, we divide partial waves into two groups: waves with $\mathrm{Im}(k_{yn}/\omega) > 0$ and $\mathrm{Im}(k_{yn}/\omega) < 0$. Next, in each group, we can identify four loops using computed values of $\mathrm{Re}(k_{yn}/\omega)$, $\mathrm{Im}(k_{yn}/\omega)$ and power flow angle (PFA) along the integral path. Then, we choose the loop with $0 < \mathrm{Im}(k_{yn}/\omega)$ along the integral path and the minimum value of $|\mathrm{Im}(k_{yn}/\omega)|$ at two sampling points $c = N_s/2$ and $c = N_s$ for the propagating wave. When the preceding step gives two loops, we must exam each loop for computing the NEP. Finally, we choose three loops with $\mathrm{Im}(k_{yn}/\omega) > 0$ for attenuation waves.

For computing SAWs, we choose four partial waves with $\mathrm{Im}(k_{yn}/\omega) > 0$.

5. Numerical results

The contour integral methods, SSM and (9), are implemented in Matlab without parallel computing toolbox and run in double precision arithmetic. The order of moment and block are $M = 1$ and $L = 4$ in the SSM. The center $o = (e_1 + e_2)/2$ and radius $\rho = (e_1 - e_2)/2$ of the circle as the integral path are specified by two endpoints of the diameter $(e_1,\ e_2)$.

Figs 1 and **2** show k_{yn}/ω or P_y for 175° rot. *Y-X* $\mathrm{LiNbO_3}$ using $(e_1,\ e_2) = (1/4080,\ 1/4700)$ s/m and $(1/3650,\ 1/4050)$ s/m, respectively, and $N_s = 32$. Presented algorithm choose proper partial waves: for LSAW analysis, the green solid line in Fig. 1(a) and the red, blue, and black solid lines in Fig. 1(b) are chosen. For slow LSAW analysis, we have two groups, solid and broken lines in Fig. 2(b). Next, we choose the blue and red lines in Fig. 2(a), then the black line in Fig. 2(b), finally the green line. For SAW analysis, four solid lines in Fig. 2(b) are chosen.

Fig . 3 shows complex velocity for θ° rot. *Y-X* $\mathrm{LiNbO_3}$ substrate. In the SSM and (9), we used $N_s = 32$. For SAW analysis, we used (1/3050, 1/4050) s/m. For analyses of fast and slow Leaky SAWs in free-surface substrate, (1/3850, 1/4060) s/m and (1/4080, 1/4700) s/m were used, respectively, and we use, in metallized surface substrate, (1/3850, 1/4000) s/m and (1/4080, 1/4480) s/m. In the vicinity of the quasishear wave velocity that is a branch point in the complex inverse velocity plane, the SSM requires larger N_s or smaller ρ for decreasing numerical instability caused by contribution of the branch point. In addition, with increasing attenuation, the location of the eigenvalue comes closer to the integral path and the SSM requires larger N_s or o having small imaginaly part. Therefore, we used (1/4700, 1/4792) s/m for free-surface substrate and for metallized surface substrate $(1/3860 - \mathrm{j}4 \times 10^{-6},\ 1/4060 - \mathrm{j}4 \times 10^{-6})$ s/m and $(1/4080 - \mathrm{j}4 \times 10^{-6}, 1/4480 - \mathrm{j}4 \times 10^{-6})$ s/m. Because smaller ρ is used, we used $N_s = 16$. For FEM analysis, we used Comsol Multiphysics. The value of $\widehat{M}_{\mathrm{eig}}$ is 1 for all Leaky SAW/SAW velocity computation.

Fig. 3 and $\widehat{M}_{\mathrm{eig}}$ being 1 show the validity of presented analysis.

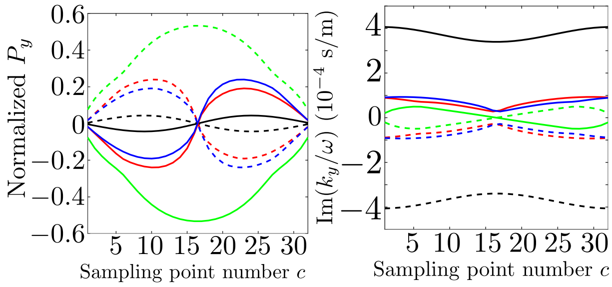

(a) Normalized P_y (b) $\mathrm{Im}(k_y/\omega)$

Fig. 1 Indices for choosing partial waves for LSAW

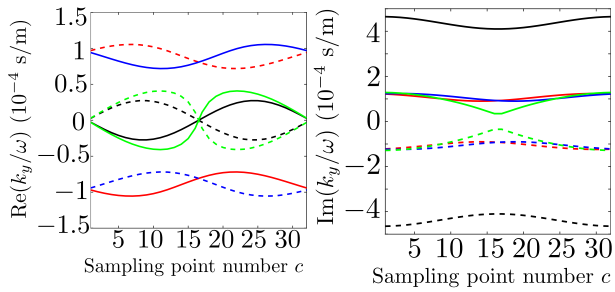

(a) $\mathrm{Re}(k_y/\omega)$ (b) $\mathrm{Im}(k_y/\omega)$

Fig. 2 Indices for choosing partial waves for slow LSAW and SAW

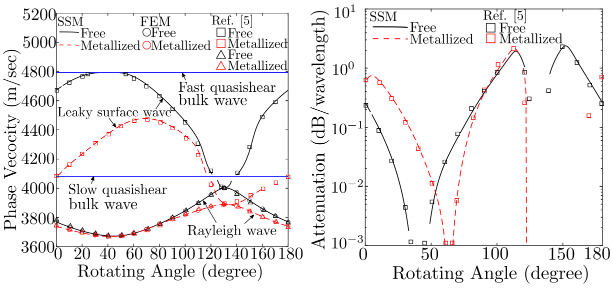

(a) Phase velocity (b) Attenuation

Fig. 3 Computed complex velocity for θ°rot. *Y-X* $\mathrm{LiNbO_3}$

References

1. E. L. Adler: IEEE Trans. Ultrason., Ferroelect., Freq. Contr., **37**(1990) 485.
2. E. L. Adler: IEEE Trans. Ultrason., Ferroelect., Freq. Contr., **41**(1994) 699.
3. Y. Maeda, Y. Futamura and T. Sakurai: JSIAM Letters, **3** (2011) 61.
4. J. Asakura, T. Sakurai, H. Tadano, T. Ikegami and K. Kimura: JSIAM Letters, **1** (2009) 52.
5. K. Yamanouchi and K. Shibayama: J. Appl. Phys., **43** (1972) 856